Lawrence Berkeley National Laboratory
Energy Storage & Distributed Resources

Title
Strength, toughness, and reliability of a porous glass/biopolymer composite scaffold

Permalink
https://escholarship.org/uc/item/98t0b6b7

Journal
Journal of Biomedical Materials Research Part B Applied Biomaterials, 106(3)

ISSN
1552-4973

Authors
Fu, Qiang
Jia, Weitao
Lau, Grace Y
et al.

Publication Date
2018-04-01

DOI
10.1002/jbm.b.33924

Peer reviewed

Strength, Toughness and Reliability of a Porous Glass/ Biopolymer Composite Scaffold

Qiang Fu[1], **Weitao Jia**[2], **Grace Y Lau**[1], and **Antoni P. Tomsia**[1]

[1]Materials Sciences Division, Lawrence Berkeley National Laboratory, Berkeley, CA 94720

[2]Department of Orthopedic Surgery, Shanghai Jiaotong University Affiliated Sixth People's Hospital, Shanghai 200233, China

Abstract

Development of bioactive glass and ceramic scaffolds intended for the reconstruction of large segmental bone defects remains a challenge for materials science due to the complexities involved in clinical implantation, bone-implant reaction, implant degradation and the multiple loading modes the implants subjected to. A comprehensive evaluation of the mechanical properties of inorganic scaffolds and exploration of new ways to toughen brittle constructs are critical prior to their successful application in loaded sites. A simple and widely adopted approach involves the coating of an inorganic scaffold with a polymeric material. In this work, a systematic evaluation of the influence of a biopolymer, polycaprolactone (PCL), coating on the mechanical performance of bioactive glass scaffolds was carried out. Results from this work indicate that a biopolymer PCL coating was more effective in increasing the compressive strength and reliability of the glass scaffold under compression, but less effective in improving its flexural strength or fracture toughness. This is the first report that reveals the limited successfulness of a polymer coating in improving the toughness of strong scaffolds, suggesting that new and novel ways of toughening inorganic scaffolds should be future research directions for scaffolds applied in loaded sites.

Keywords

Mechanical strength; Fracture toughness; reliability; bioactive glass scaffold; polymeric coating

1. Introduction

The repair of large segmental bone defects resulting from trauma, inflammation and pathology is a common yet challenging clinical problem [1,2]. Despite high success rate of traditional autograft and allograft approaches, they both suffer from limitations such as donor site morbidity, limited supply, possible transmission of diseases, and high costs [3–7]. Recent clinical practices using a tissue engineering approach by implanting a bone marrow stroma-seeded porous hydroxyapatite (HA) scaffold in patient long bone defects (4–6 cm in length) demonstrate a significant improvement in the repair of load-bearing bone sites [1,8,9]. A complete fusion between the implant and the host bone is found 5 to 7 months after

Correspondence to: Qiang Fu.

surgery and good integration is maintained in all the follow-ups (up to 7 years postsurgery) [8]. However, the low resorption rate of porous HA scaffolds and low mechanical strength are among the challenges for their uses in clinical practices [8]. The development of resorbable constructs with high mechanical strength is a prerequisite prior to their extensive applications in clinical practices.

In addition to calcium phosphate-based bioactive ceramics, bioactive glass also has received wide interest as an attractive scaffold material due to its excellent bioactivity, controllable degradation rate and ease in densification via a viscous flow sintering [10,11]. Recent progress in the advanced fabrication techniques such as freeze casting and solid freeform fabrication (SFF) is paving the way to the development of highly strong and porous glass scaffolds that can be applied to load-bearing sites [12–15]. Utilizing a direct ink writing technique, glass scaffolds with a compressive strength in the range of both trabecular and cortical bones are successfully created [12,13,16–19]. Considering the complexity of the loading modes during normal physiological activities, a simple measure of the compressive strength of scaffolds is not sufficient to evaluate their mechanical performances for application in loaded bone sites. However, in most cases this is not well appreciated by material scientists/researchers who generally take compressive strength as a primary screening test for scaffold selection [12,20].

Additionally, bioactive glass and ceramic scaffolds are brittle, so the quantification of their brittle behavior and evaluation of their mechanical reliability are also of importance. Attempts have been made toward the development of tough composite scaffolds by coating bioactive glass and ceramic scaffolds with a thin biodegradable polymer such as poly(D,L-lactic acid), PDLLA, poly(3-hydroxybutyrate), P(3HB), alginate, polycaprolactone, PCL, and polyvinyl-alcohol, PVA [21–27]. The work of fracture of the coated scaffolds is found to be significantly improved due to the presence of fibril extension and crack bridging. However, unlike fracture toughness, work of fracture is not a true materials property and can only be used for comparison within a given study. Furthermore, the scaffolds in the reported studies are fabricated using a polymer foam replication technique, which generally produces weak scaffolds intended for non-loaded bone sites [21–25,28]. The successfulness of polymer coatings in toughening strong scaffolds (strength close or comparable to that of human cortical bone) remains unclear.

In this work, a comprehensive evaluation of the impact of a polymer coating, PCL, on the mechanical performances of a periodic bioactive glass (13–93) scaffold prepared by a direct ink writing technique was carried out. Mechanical properties including compressive strength, flexural strength and fracture toughness were measured, while their mechanical reliability was analyzed using a Weibull distribution.

2. Experimental Section

2.1 Preparation of glass scaffolds

Scaffolds of 13–93 glass (composition (wt%): 53% SiO_2, 6% Na_2O, 12% K_2O; 5% MgO, 20% CaO, and 4% P_2O_5) were prepared using a direct ink writing technique described in detail elsewhere [13,16]. In brief, glass inks containing 40 vol% particles were prepared by mixing glass particles in a 20 wt% Pluronic® F-127 solution with water as a solvent and

homogenized at 0°C for 12 hours. Glass scaffolds were fabricated by printing the inks through a 250 μm nozzle (EFD precision tips, EFD, East Providence, RI) using a robotic deposition device (RoboCAD 3.0, 3-D Inks, Stillwater, OK). After printing, the scaffolds were air-dried for 24 hours and subjected to a controlled heat treatment to decompose the organics and sinter the glass particle into dense rods. The green samples were heated at 1°C/min to 600°C in flowing O_2 gas, and then at 5°C/min to 700°C, and kept for one hour.

To determine the impact of a biopolymer coating on the mechanical performances of the sintered glass scaffold, a thin PCL coating was applied by infiltrating the polished scaffold four times with a 5.0% PCL in 1,4-dioxane. After infiltration, samples were placed on a Kimwipes® paper to remove the excess solution and dry in air.

2.2 Characterization of glass scaffolds

The porosity of the as-sintered and PCL-coated glass scaffolds was measured using the Archimedes method. Scanning electron microscopy, SEM, (Hitachi S-4300, Tokyo, Japan) was used to observe the microstructure of the scaffolds. The samples were sputter-coated with Au and examined at an accelerating voltage of 10 kV.

Synchrotron X-ray micro-computed tomography (SR microCT) was used to obtain a 3-D perspective of the scaffold. Scanning was conducted at the Advanced Light Source (ALS-LBNL, Berkeley, CA) with 22 keV monochromatic X-rays and a 4.4 μm voxel size (resolution). The data sets were reconstructed using the software Octopus and the 3-D visualization was performed using Avizo™ software.

2.3 Mechanical performances

The compressive strength of the glass scaffolds was measured by performing uniaxial tests on cubic blocks (3 × 3 × 3 mm) cut from the sintered specimens using a low-speed diamond saw. Surface grinding was conducted on the blocks to ensure that the two tested ends were flat and parallel. Polished specimens were checked using an optical microscope to make sure surfaces are free of visible flaws. Samples were compressed in the direction parallel to the pore orientation on a servo-hydraulic testing machine (MTS810, MTS Systems, Eden Prairie, MN) at a crosshead speed of 0.5 mm/min. Twenty samples were tested to get statistically reliable values for each group and three replica groups were measured.

The flexural strength was measured using a three-point bending method. Beam specimens (3×3×25 mm) were cut from a large sample using a low-speed diamond saw and finished on a surface grinder. Strength tests used a support span L of 15 mm and a crosshead speed of 0.5 mm/min in general accordance with the American Society for Testing and Materials (ASTM) standard [29]. Similar as compressive testing, the load was applied in the direction parallel to the pore orientation for bending tests. Same number of test specimens were used as those for compressive strength measurement.

Fracture toughness, K_{IC}, was determined using the three-point bending test on single edge notched beam (SENB) specimens (3 × 3 × 25 mm) over a 15 mm span. A thin notch (< 200 μm) of approximately 1.3 mm deep was machined at the midpoint of one 25 mm edge according to a procedure specified by an ASTM standard [30]. The notch was made

perpendicular to the pore orientation and through the rods rather than in the middle of a single rod to reduce the variations for the test. The load was applied in the direction parallel to the pore orientation. Samples were tested with a crosshead speed of 0.5 mm/min, in general accordance with an ASTM standard [30]. Fracture toughnes, K_{IC}, is determined by the following equation:

$$K_{IC} = g\left(\frac{P_{\max} S_0 10^{-6}}{BW^{3/2}}\right)\left[\frac{3(a/W)^{1/2}}{2(1-a/W)^{3/2}}\right] \quad (3)$$

where a is the crack (or notch) length, W is the top to bottom dimension of the test specimen parallel to the crack length (depth), g is the function of the ratio a/W for three-point flexure [30], P_{max} is the maximum force applied, S_0 is the outer span is the specimens, and B is the side to side dimension of the test specimen perpendicular to the crack length.

The reliability or the probability of failure of brittle materials is quantified by a probability function proposed by Weibull and specified by ASTM [31,32], which is applicable to failure occurring from critical flaws. The Weibull distribution is given as a cumulative distribution function [31,32]:

$$P_f = 1 - \exp\left[-\left(\frac{\sigma}{\sigma_\theta}\right)^m\right] \quad (1)$$

where P_f is the probability of failure at a stress σ, σ_θ is Weibull characteristic strength, and m is the Weibull modulus (or the shape parameter). Weibull modulus, m, is obtained from the plot of $ln[-ln(1-p)]$ versus $ln\sigma$, the slope of which gives the m value. A higher Weibull modulus indicates a tight strength distribution and therefore a more reliable material. Characteristics strength, σ_θ, is estimated to be the strength that corresponds to a P_f of 63.2%, or a value zero for $ln[-ln(1-p)]$.

To evaluate P_f the following equation is used [32]:

$$P_f(\sigma_i) = \frac{i - 0.5}{N} \quad (2)$$

where N is the total number of specimens tested and i is the specimen rank in ascending order of failure stress. To get an unbiased estimate of the failure probability, the recommended number of specimens is between 20 and 30 [32–34].

Statistical analysis was performed on test results with one-way analysis of variance(ANOVA) followed by a Tukey's *post hoc* test, with the level of significance set at p < 0.05.

3. Results

3.1 Scaffold microstructure

A 3-dimensional visualization of the scaffold reveals a periodic structure composed of a sintered glass lattice and interconnected open porosity (Figure 1a). Two types of pores were observed in the scaffolds: large square pores with a width of 200 μm within each layer and small rectangular pores of 200 × 60 μm between adjacent layers (Figure 1b and c). A smooth strut surface with few closed pores was observed, indicating the densification via a viscous flow sintering. An open porosity of 50% ± 5 was measured using the Archimedes method. After applying a thin PCL coating, no noticeable change in microstructure or porosity was observed in coated scaffolds compared with those without coating (Figure 2). Small pores (< 20 μm) on surfaces were filled with PCL while larger pores remained open (Figure 2b). The thickness of the PCL coating was less than one micron based on the measurement of the fractured cross sections in coated samples.

3.2 Mechanical strength and reliability

Compressive and flexural strengths of 13–93 glass scaffolds with and without PCL coating were tested. The stress-strain curve of the scaffolds under compression is shown in Figure 3. The data are engineering stresses and strains, based on the initial cross-sectional area and length of the test sample, and do not represent the true stresses and strains. Due to the small sample geometry (3 × 3 × 3 mm) there were seven unit cells in the shortest dimension. However, the strength values from this work were compared to those obtained on cylinder specimens (8 mm in diameter × 10 mm in length) [35], indicating the sample geometry did not have a big impact on the strength in this glass scaffold.

A typical brittle behavior with a catastrophic failure mode was observed for the 13–93 glass scaffold under compression. On the other hand, PCL-coated scaffold shows a gradual failure mode with a high strain tolerance. The coated scaffold held its shape after the peak stress was achieved. No shatter of the scaffold was observed and the increasing compression load at above 70% strain was due to the densification of the scaffold.

Two trends were observed in the stress-strain curve under compression. First, the peak strength of the PLC-coated scaffolds was about 25% higher than that of uncoated scaffold. The stretching of PCL fibril observed in the fractured scaffold were indications of its crack shielding effect (Figure 3b). Second, the work of fracture (area under the stress-strain curve) of the PCL-coated glass scaffold (calculated based on 5% strain) was about 4 times that of the uncoated scaffold, indicating the creation of a relatively tougher composite scaffold. The stretched PCL fibril also helped keep the shape of the broken scaffold, which improved its toughness under compression load.

The influence of the PCL coating on the compressive strength of 13–93 glass scaffold is more clearly evidenced in Figure 4, which shows the Weibull strength distributions and logarithmic plots for compression. A tighter strength distribution and increased Weibull characteristic strength (the strength corresponding to a P_f of 63.2%) from 80 ± 10 to 102 ± 11 MPa were observed in Figure 4a. Furthermore, the Weibull modulus, 6.0 ± 0.5 for uncoated and 13.0 ± 1.0 for PCL-coated glass scaffold, was doubled by applying a surface

polymeric coating (Figure 4b), indicating a much higher reliability of the latter. The strength values are much higher than those fabricated using traditional techniques, such as sol-gel, polymer foam replication and porogen, which generally fall within the range of that for trabecular bone (2–12 MPa) [12]. The compressive strengths are also close to or in the lower range of cortical bone (100–150 MPa), indicating their potential applications in load-bearing sites (Figure 5).

The stress-strain curve of PCL-coated and uncoated glass scaffold under bending is shown in Figure 6a. Both scaffolds exhibited a brittle behavior with a catastrophic failure after peak load under bending. The PCL coating did not significantly improve the brittle failure behavior, although the work of fracture was increased by 4 times. The stretching of PCL fibril was also observed as shown in Figure 6b, similar to those present during the compression of the scaffold (Figure 3b). However, this thin polymeric coating (1 μm) showed little success in increasing the strength or reliability of scaffold under bending. A comparable Weibull strength distribution was observed for both uncoated and PCL-coated scaffolds with a characteristic flexural strength of 40 ± 5 and 41 ± 6 MPa (Figure 7a). The Weibull modulus, determined from the slope of the logarithmic plots for bending, was 5.3 ± 0.4 and 5.6 ± 0.5 for uncoated and PCL-coated scaffold, respectively (Figure 7b). The flexural strength values (40 MPa) are much higher than those fabricated using traditional techniques, such as sol-gel, polymer foam replication and porogen, which generally fall within the range of that for trabecular bone (10–20 MPa) [12,20]. However, they are also much lower than that of cortical bone (135–193 MPa) (Figure 8). A summary of the mechanical properties of both scaffolds is listed in Table 1.

3.3 Fracture toughness

Fracture toughness of brittle porous materials is analyzed using a continuum linear elastic solution for the stress field in front of a crack tip by assuming that crack length is much larger than the cell size [36,37]. The fracture toughness, K_{IC}, of both uncoated and PCL-coated scaffolds were tested on pre-cracked beam test specimens and calculated using Equation (3), in accordance with ASTM [30].

The K_{IC} values for both scaffolds were essentially the same, 0.8 ± 0.2 MPa·m$^{1/2}$, which is in the range of values for glass (0.5–1 MPa·m$^{1/2}$). In the uncoated scaffold, the cracks followed a tortuous path and tend to propagate along the joints of adjacent glass struts (Figure 9b), which was the weakest part in the scaffold. The load from prior layer(s) of the struts during scaffold preparation resulted in the deformation of the glass rods close to the joints (as indicated by the white arrows in Figure 9a), which led to the formation of a weak interface and an easy path for the crack propagation. A similar tortuous crack path was observed in the PCL-coated scaffold after three-point bending test (Figure 9c). Although crack bridging was observed in some fractured samples (Figure 9c and d), the thin PCL film did not show significant toughening to the scaffold.

4. Discussion

For bone tissue engineering, both pore size and pore interconnectivity in scaffolds are critical factors for cell adhesion, bone ingrowth and nutrient delivery, as indicated by animal

studies and clinical practice [1,9,38]. Scaffolds composed of interconnected porosity with a mean diameter or width of 100 μm or greater and open porosity >50% are generally considered as the minimum requirements for the repair and reconstruction of bone defects [39–41]. The pore size and pore interconnectivity in the glass scaffolds from this work are satisfactory with regard to its application in the reconstruction of long-bone defects (Figure 1). To improve the toughness of brittle inorganic scaffolds, biopolymers are generally combined with the inorganic materials to make a composite scaffold. The biopolymers like PDLLA and PCL are approved by the Food and Drug Administration (FDA) for clinical applications, so their biocompatibility is not a concern. Both in vitro and in vivo work indicates the incorporation of PCL does not significantly impact the bioactivity of the inorganic scaffolds [19,42–45].

In this work, the impact of a PCL coating on the strength, mechanical reliability and fracture toughness of a bioactive 13–93 glass scaffold was investigated. All the mechanical tests in this work were conducted by applying loads in the direction parallel to the pore orientation, which was reported to produce a strength about 2.5 times the value when tested perpendicularly in a bioactive glass scaffold [13,16]. The PCL coating was found to be effective in filling small pores on the surfaces of rods, and improving the strength and reliability of the glass scaffold under compression. However, the improvement on the flexural strength and reliability provided by the polymeric coating was minimal. These findings are not all consistent with literature work. In particular, the limited capability of PLC coating to increase the flexural strength is a first report in composite scaffolds. The improvement in compressive strength and reliability (Weibull modulus) correspond well with the ability of the PCL coating to fill some micro pores and possibly micro cracks present at the surface of glass rods (Figure 2). In addition, the stretched polymer fibril was able to keep the shape of the scaffold and lead to an increased work of fracture. These findings, small increase in compressive strength and significant improvement in work of fracture, were in good agreement with reported studies [12,23,46]. By coating a biphasic calcium phosphate (BCP) scaffold with PCL, the compressive strength of macroporous BCP scaffold is increased from 15.6 to 17.8 MPa and strain energy density (work of fracture) is increased up to 10 times [46]. The higher work of fracture is attributed to the toughening by crack bridging by polymer fibrils. In another study, a poly(D,L-lacticacid) (PDLLA) coating on a Bioglass®-based scaffold results in the increase of its compressive strength from 0.1–0.4 to 0.2–0.7 MPa [22]. However, it should be noted that most of the literature work is conducted on glass and ceramic scaffolds composed of rods containing open porosity due to incomplete densification. The micro pores in their rods result in a low mechanical strength, generally in the range of that for trabecular bone. The formation of interpenetrating polymer-ceramic microstructure can be achieved in this type of scaffolds due to the presence of micro pores [25,28]. In contrast, the polymer infiltration into the inner part of rods cannot be obtained in this work due to the densification of glass rods resulting from viscous flow sintering of the glass powders, as shown in Figure 1. The polymer coating was applied only to the surface of the rods with no deep penetration because of the lack of the micro porosity in the densified struts, which makes the toughening mechanism such as polymer fibril bridging observed in scaffolds with micro pores less effective [31]. The limited improvement on flexural strength and reliability indicates a thin PCL coating was not effective to prevent

crack propagation in the scaffold under a tensile stress and the strength is mainly determined by the intrinsic property of the rods.

Comparable fracture toughness values for both uncoated and PCL-coated glass scaffolds provide additional evidence that a thin polymer coating is not effective in improving the toughness of a brittle scaffold. This is contrary to the general recognition that the fracture toughness of a porous glass or ceramic scaffold can be significantly improved by coating or infiltration with a biodegradable polymer [21–24,46,47]. The increasing work of fracture in compression and bending test is reported and considered as an indication of the creation of "toughened" composite scaffold in literature [25]. However, the results in this work reveal the true fracture toughness is not be increased by a thin polymer coating. The increase of work of fracture in compression or bending test observed in literature is most likely attributed to the improved mechanical reliability resulting from elimination of micro cracks or micro pores.

It should be noted that both flexural strength and fracture toughness were tested on specimens prepared in accordance with ASTM test methods based on dense ceramic materials, while porosity is required in scaffolds. In both tests, less than 10 unit cells were present in the shortest dimension, which may have negative impact on the tested values.

Although a polymer coating on the surface of scaffolds is not an effective way to improve toughness of brittle ceramic materials, efforts are being made to explore new and novel approaches to develop tough organic/inorganic composites [11,48–55]. With the inspiration from mineralized composites such as bone, dentin and nacre, engineered polymer/ceramic composites with a "brick and mortar" structure and high fracture toughness similar to that of nacre were developed [48]. Additionally, sol-gel hybrid scaffolds were developed by introducing a degradable polymer in the sol stage to form interlocking polymer chains at molecular level [11]. Despite these advances, compromises always have to be made amongst porosity, strength, bioactivity and degradation, especially for scaffolds intended for use at loaded sites.

5. Conclusions

The influence of a biopolymer, polycaprolactone (PCL), on the mechanical performance of the bioactive 13–93 glass scaffold prepared using a direct ink writing technique was investigated. Both compressive strength and reliability of the glass scaffold were improved by applying a thin coating on its surface, which may be due to the filling of the micro pores and micro cracks on the glass struts. However, no significant improvement in flexural strength and fracture toughness was observed, suggesting that a thin polymeric coating was not able to provide sufficient toughening mechanisms. Results from this work reveal that a polymer coating is more effective in increasing the scaffold strength and reliability in compression but less effective in improving its flexural strength or toughness.

Acknowledgments

References

1. Cancedda R, Giannoni P, Mastrogiacomo M. A tissue engineering approach to bone repair in large animal models and in clinical practice. Biomaterials. 2007; 28(29):4240–4250. [PubMed: 17644173]

2. Kong Y-Y, Feige U, Sarosi I, Bolon B, Tafuri A, Morony S, Capparelli C, Li J, Elliott R, McCabe S. Activated T cells regulate bone loss and joint destruction in adjuvant arthritis through osteoprotegerin ligand. Nature. 1999; 402:43–47.

3. Enneking WF, Eady JL, Burchardt H. Autogenous Cortical Bone-Grafts in the Reconstruction of Segmental Skeletal Defects. Journal of Bone and Joint Surgery-American Volume. 1980; 62(7): 1039–1058.

4. Taylor GI. The Current Status of Free Vascularized Bone-Grafts. Clinics in Plastic Surgery. 1983; 10(1):185–209. [PubMed: 6340912]

5. Weiland AJ, Moore JR, Daniel RK. Vascularized Bone Autografts - Experience with 41 Cases. Clinical Orthopaedics and Related Research. 1983; (174):87–95.

6. Stevenson S. The Immune-Response to Osteochondral Allografts in Dogs. Journal of Bone and Joint Surgery-American Volume. 1987; 69A(4):573–582.

7. Lord CF, Gebhardt MC, Tomford WW, Mankin HJ. Infection in Bone Allografts - Incidence, Nature, and Treatment. Journal of Bone and Joint Surgery-American Volume. 1988; 70A(3):369–376.

8. Marcacci M, Kon E, Moukhachev V, Lavroukov A, Kutepov S, Quarto R, Mastrogiacomo M, Cancedda R. Stem cells associated with macroporous bioceramics for long bone repair: 6-to 7-year outcome of a pilot clinical study. Tissue engineering. 2007; 13(5):947–955. [PubMed: 17484701]

9. Quarto R, Mastrogiacomo M, Cancedda R, Kutepov SM, Mukhachev V, Lavroukov A, Kon E, Marcacci M. Repair of large bone defects with the use of autologous bone marrow stromal cells. New England Journal of Medicine. 2001; 344(5):385–386. [PubMed: 11195802]

10. Rahaman MN, Day DE, Bal BS, Fu Q, Jung SB, Bonewald LF, Tomsia AP. Bioactive glass in tissue engineering. Acta Biomater. 2011; 7(6):2355–73. [PubMed: 21421084]

11. Jones JR. Review of bioactive glass: From Hench to hybrids. Acta Biomaterialia. 2013; 9(1):4457–4486. [PubMed: 22922331]

12. Fu Q, Saiz E, Rahaman MN, Tomsia AP. Bioactive glass scaffolds for bone tissue engineering: state of the art and future perspectives. Mater Sci Eng C Mater Biol Appl. 2011; 31(7):1245–1256. [PubMed: 21912447]

13. Fu Q, Saiz E, Tomsia AP. Bio-inspired Highly Porous and Strong Glass Scaffolds. Adv Funct Mater. 2011; 21:1058–1063. [PubMed: 21544222]

14. Fu Q, Saiz E, Rahaman MN, Tomsia AP. Toward Strong and Tough Glass and Ceramic Scaffolds for Bone Repair. Advanced Functional Materials. 2013; 23(44):5461–5467.

15. Liu X, Rahaman MN, Hilmas GE, Bal BS. Mechanical properties of bioactive glass (13–93) scaffolds fabricated by robotic deposition for structural bone repair. Acta Biomaterialia. 2013; 9(6):7025–7034. [PubMed: 23438862]

16. Fu Q, Saiz E, Tomsia AP. Direct ink writing of highly porous and strong glass scaffolds for load-bearing bone defects repair and regeneration. Acta Biomaterialia. 2011; 7(10):3547–3554. [PubMed: 21745606]

17. Deliormanli AM, Rahaman MN. Direct-write assembly of silicate and borate bioactive glass scaffolds for bone repair. Journal of the European Ceramic Society. 2012; 32(14):3637–3646.

18. Wu C, Luo Y, Cuniberti G, Xiao Y, Gelinsky M. Three-dimensional printing of hierarchical and tough mesoporous bioactive glass scaffolds with a controllable pore architecture, excellent mechanical strength and mineralization ability. Acta Biomaterialia. 2011; 7(6):2644–2650. [PubMed: 21402182]

19. Poh PS, Hutmacher DW, Stevens MM, Woodruff MA. Fabrication and in vitro characterization of bioactive glass composite scaffolds for bone regeneration. Biofabrication. 2013; 5(4):045005. [PubMed: 24192136]

20. Fu Q, Saiz E, Rahaman MN, Tomsia AP. Toward strong and tough glass and ceramic scaffolds for bone repair. Advanced Functional Materials. 2013; 23(44):5461–5476.

21. Chen QZ, Boccaccini AR. Poly(D,L-lactic acid) coated 45S5 Bioglass®-based scaffolds: Processing and characterization. Journal of Biomedical Materials Research Part A. 2006; 77A(3): 445–457.

22. Bretcanu O, Misra S, Roy I, Renghini C, Fiori F, Boccaccini AR, Salih V. In vitro biocompatibility of 45S5 Bioglass ®-derived glass-ceramic scaffolds coated with poly(3-hydroxybutyrate). Journal of Tissue Engineering and Regenerative Medicine. 2009; 3(2):139–148. [PubMed: 19170250]

23. Mantsos T, Chatzistavrou X, Roether JA, Hupa L, Arstila H, Boccaccini AR. Non-crystalline composite tissue engineering scaffolds using boron-containing bioactive glass and poly(D,L-lactic acid) coatings. Biomedical Materials. 2009; 4(5):055002. [PubMed: 19776493]

24. Mourino V, Newby P, Boccaccini AR. Preparation and Characterization of Gallium Releasing 3-D Alginate Coated 45S5 Bioglass ® Based Scaffolds for Bone Tissue Engineering. Advanced Engineering Materials. 2010; 12(7):B283–B291.

25. Yunos DM, Bretcanu O, Boccaccini AR. Polymer-bioceramic composites for tissue engineering scaffolds. Journal of Materials Science. 2008; 43(13):4433–4442.

26. Wagoner Johnson AJ, Herschler BA. A review of the mechanical behavior of CaP and CaP/polymer composites for applications in bone replacement and repair. Acta Biomaterialia. 2011; 7(1):16–30. [PubMed: 20655397]

27. Bertolla L, Dlouhý I, Philippart A, Boccaccini A. Mechanical reinforcement of Bioglass®-based scaffolds by novel polyvinyl-alcohol/microfibrillated cellulose composite coating. Materials Letters. 2014; 118:204–207.

28. Martínez-Vázquez FJ, Miranda P, Guiberteau F, Pajares A. Reinforcing bioceramic scaffolds with in situ synthesized ε-polycaprolactone coatings. Journal of Biomedical Materials Research Part A. 2013; 101(12):3551–3559. [PubMed: 23629876]

29. International A. Standard test method of flexural strength of advanced ceramics at ambient temperature. Vol. C1161-02C. West Conshohocken; Pennsylvania, USA: 2008.

30. International A. Standard Test Methods for determination of fracture toughness of advanced ceramics at ambient temperature. Vol. ASTM C1421-10. West Conshohocken; Pennsylvania, USA: 2010.

31. Weibull W. A Statistical Distribution Function of Wide Applicability. Journal of Applied Mechanics-Transactions of the Asme. 1951; 18(3):293–297.

32. International A. Standard practice for reporting uniaxial strength data and estimating Weibull distribution parameters for advanced ceramics. 2007; C1239-07

33. Bergman B. On the Estimation of the Weibull Modulus. Journal of Materials Science Letters. 1984; 3(8):689–692.

34. Sullivan JD, Lauzon PH. Experimental Probability Estimators for Weibull Plots. Journal of Materials Science Letters. 1986; 5(12):1245–1247.

35. Jia W, Fu Q, Lau GY, Huang W, Zhang C, Tomsia AP. A simple bioactive glass scaffold approach for regeneration of large segmental bone defects. Nature Communications. 2014

36. Maiti SK, Ashby MF, Gibson LJ. Fracture-Toughness of Brittle Cellular Solids. Scripta Metallurgica. 1984; 18(3):213–217.

37. Huang JS, Gibson LJ. Fracture-Toughness of Brittle Foams. Acta Metallurgica Et Materialia. 1991; 39(7):1627–1636.

38. Mastrogiacomo M, Scaglione S, Martinetti R, Dolcini L, Beltrame F, Cancedda R, Quarto R. Role of scaffold internal structure on in vivo bone formation in macroporous calcium phosphate bioceramics. Biomaterials. 2006; 27(17):3230–3237. [PubMed: 16488007]

39. Karageorgiou V, Kaplan D. Porosity of 3D biornaterial scaffolds and osteogenesis. Biomaterials. 2005; 26(27):5474–5491. [PubMed: 15860204]

40. Hulbert SF, Young FA, Mathews RS, Klawitter JJ, Talbert CD, Stelling FH. Potential of ceramic materials as permanently implantable skeletal prostheses. J Biomed Mater Res. 1970; 4:433–456. [PubMed: 5469185]

41. Hollinger JO, Brekke J, Gruskin E, Lee D. Role of bone substitutes. Clinical Orthopaedics and Related Research. 1996; (324):55–65.

42. Roohani-Esfahani SI, Dunstan CR, Davies B, Pearce S, Williams R, Zreiqat H. Repairing a critical-sized bone defect with highly porous modified and unmodified baghdadite scaffolds. Acta Biomaterialia. 2012; 8(11):4162–4172. [PubMed: 22842031]

43. Allo BA, Rizkalla AS, Mequanint K. Hydroxyapatite formation on sol-gel derived poly(ε-caprolactone)/ bioactive glass hybrid biomaterials. ACS Applied Materials and Interfaces. 2012; 4(6):3148–3156. [PubMed: 22625179]

44. Dash TK, Konkimalla VB. Poly-ε-caprolactone based formulations for drug delivery and tissue engineering: A review. Journal of Controlled Release. 2012; 158(1):15–33. [PubMed: 21963774]

45. Korpela J, Kokkari A, Korhonen H, Malin M, Närhi T, Seppälä J. Biodegradable and bioactive porous scaffold structures prepared using fused deposition modeling. Journal of Biomedical Materials Research Part B: Applied Biomaterials. 2013; 101B(4):610–619.

46. Peroglio M, Gremillard L, Gauthier C, Chazeau L, Verrier S, Alini M, Chevalier J. Mechanical properties and cytocompatibility of poly(epsilon-caprolactone)-infiltrated biphasic calcium phosphate scaffolds with bimodal pore distribution. Acta Biomaterialia. 2010; 6(11):4369–4379. [PubMed: 20553981]

47. Peroglio M, Gremillard L, Chevalier J, Chazeau L, Gauthier C, Hamaide T. Toughening of bio-ceramics scaffolds by polymer coating. Journal of the European Ceramic Society. 2007; 27(7): 2679–2685.

48. Deville S, Saiz E, Nalla RK, Tomsia AP. Freezing as a path to build complex composites. Science. 2006; 311(5760):515–518. [PubMed: 16439659]

49. Zhang J, Liu W, Schnitzler V, Tancret F, Bouler J-M. Calcium phosphate cements for bone substitution: Chemistry, handling and mechanical properties. Acta Biomaterialia. 2014; 10(3): 1035–1049. [PubMed: 24231047]

50. Galea L, Bohner M, Thuering J, Doebelin N, Aneziris CG, Graule T. Control of the size, shape and composition of highly uniform, non-agglomerated, sub-micrometer β-tricalcium phosphate and dicalcium phosphate platelets. Biomaterials. 2013; 34(27):6388–6401. [PubMed: 23755834]

51. Bohner M, Galea L, Doebelin N. Calcium phosphate bone graft substitutes: Failures and hopes. Journal of the European Ceramic Society. 2012; 32(11):2663–2671.

52. Fratzl P, Gupta HS, Paschalis EP, Roschger P. Structure and mechanical quality of the collagen-mineral nano-composite in bone. Journal of Materials Chemistry. 2004; 14(14):2115–2123.

53. Fratzl P, Weinkamer R. Nature's hierarchical materials. Progress in Materials Science. 2007; 52(8): 1263–1334.

54. Fratzl P. A composite matter of alignment. Science. 2012; 335(6065):177–178. [PubMed: 22246763]

55. Meyers MA, McKittrick J, Chen P-Y. Structural biological materials: critical mechanics-materials connections. Science. 2013; 339(6121):773–779. [PubMed: 23413348]
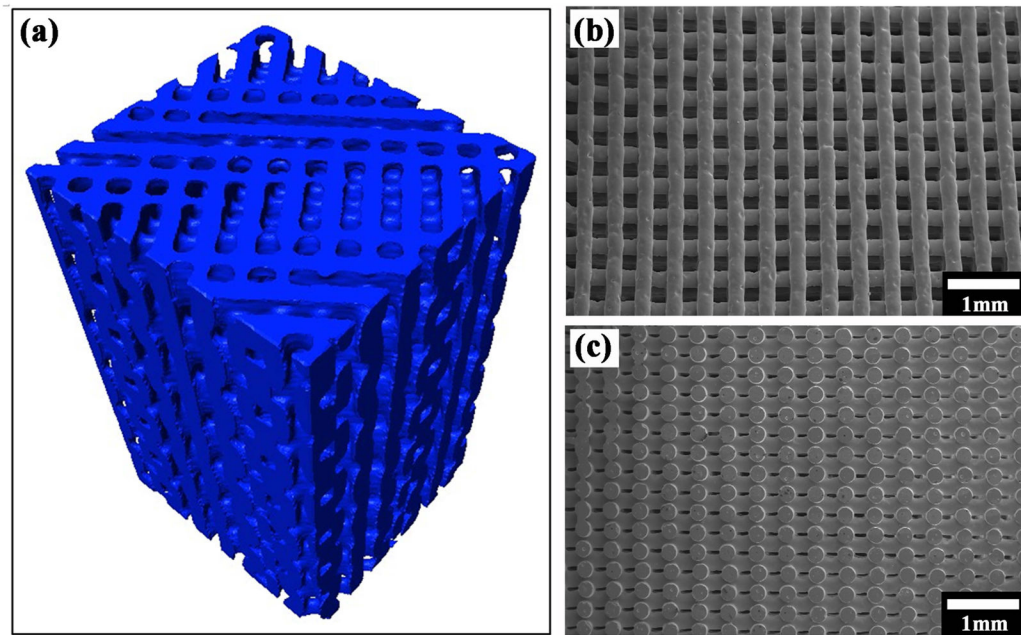
Figure 1.
Periodic bioactive glass (13–93) scaffolds created using a direct ink writing technique. (a) A 3-dimensional view of glass struts using synchrotron X-ray tomography and SEM images showing the detailed structure of the scaffold: (b) a top view of the scaffold and (c) a cross sectional view of the scaffold.
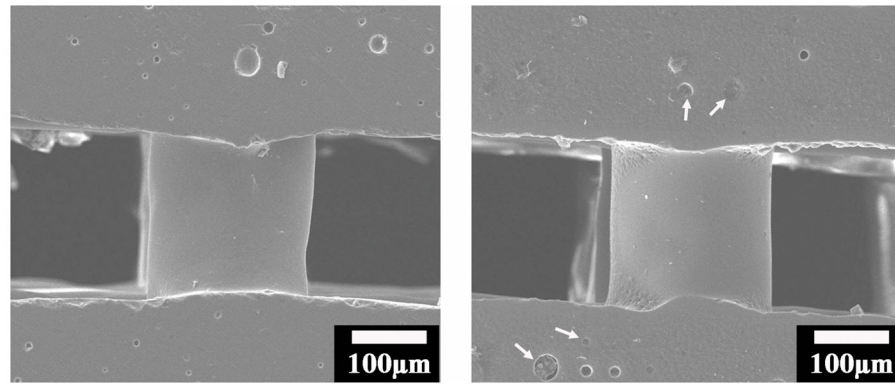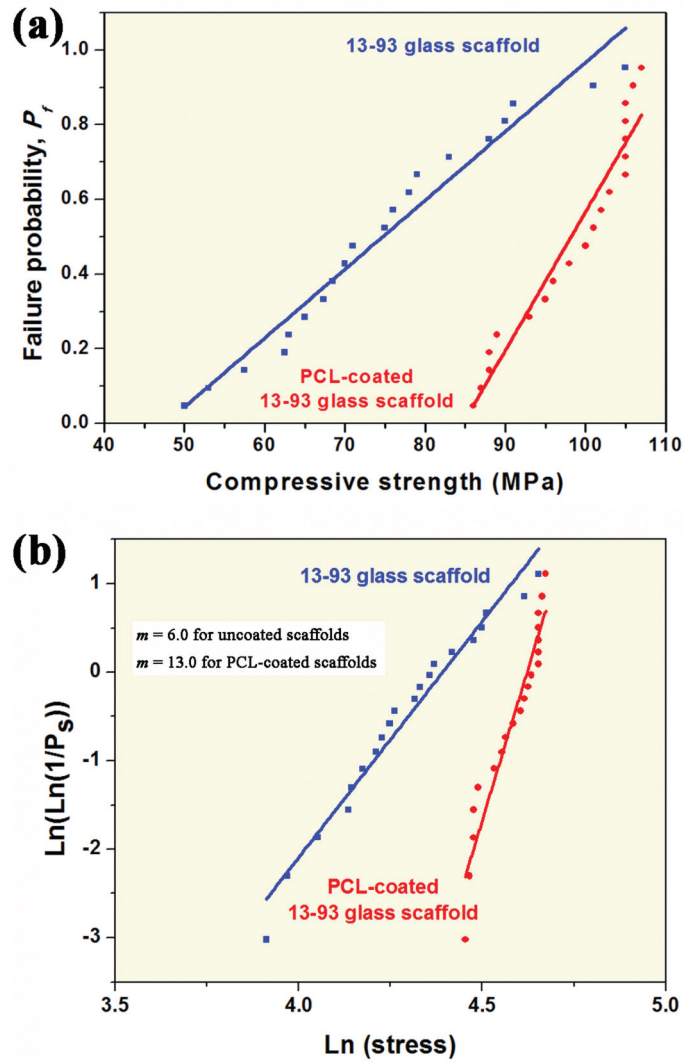
Figure 2.
SEM images showing cross sections of a bioactive glass (13–93) scaffolds: (a) polished and un-coated surfaces and (b) polished and PCL-coated surfaces. White arrows indicate the micro pores filled by the PCL coating.
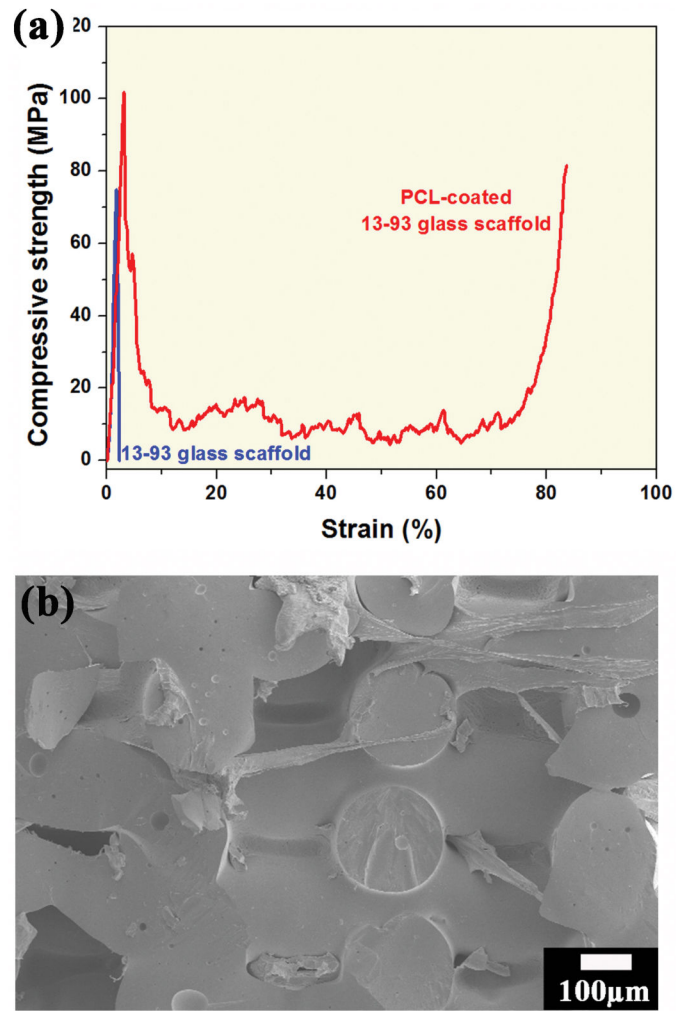
Figure 3.
(a) Stress-strain curve of the scaffold under compression along the pore orientation, inset showing the gradual failure of the PCL-coated scaffold; (b) SEM image of a fracture surface in PCL-coated scaffold after compression test.
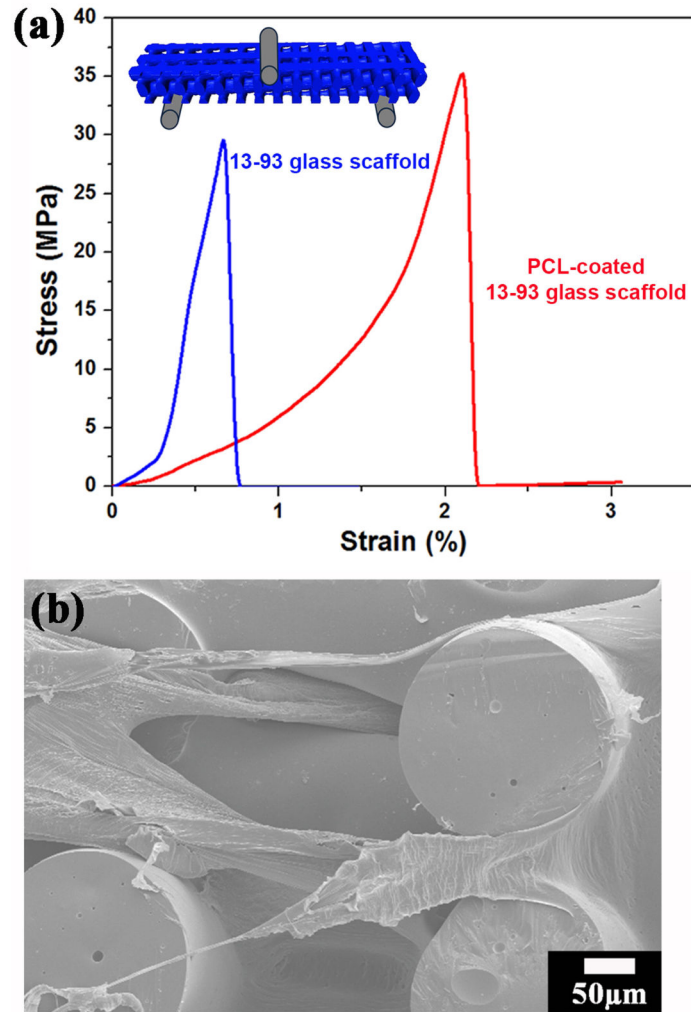
Figure 4.
(a) Weibull distribution of compressive strength of uncoated and PCL-coated glass scaffolds;
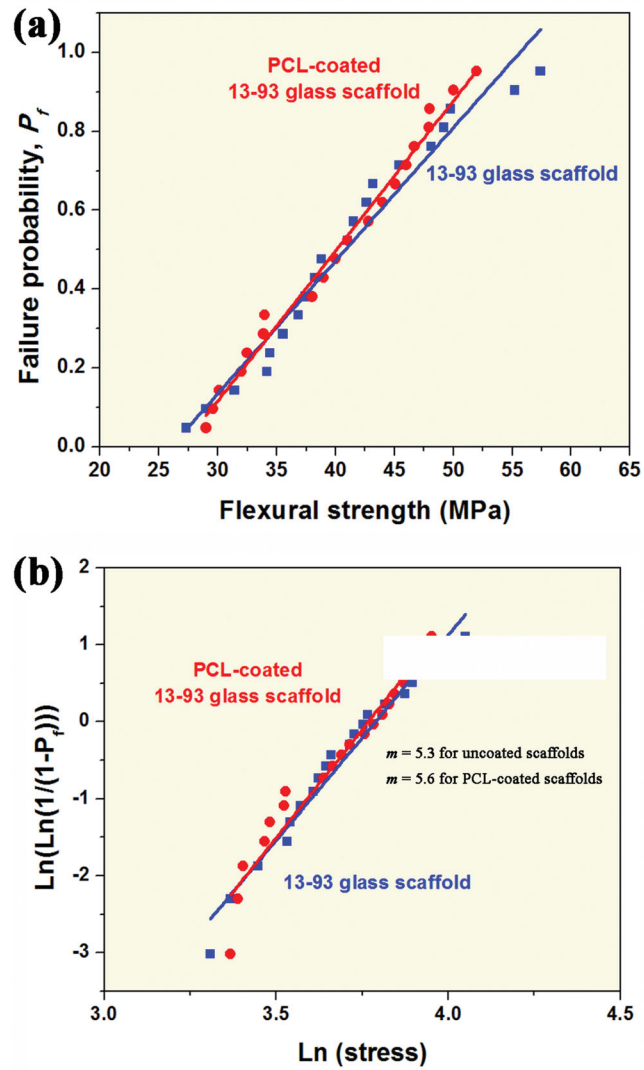(b) logarithmic plots for compressive strength values of both scaffolds.
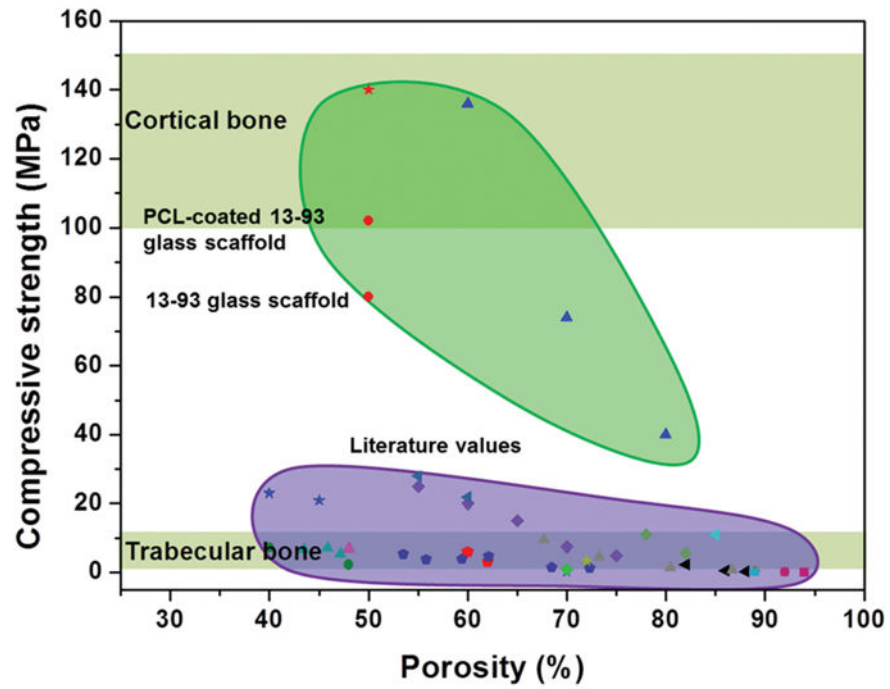
Figure 5.
A comparison of compressive strength of bioactive glass in this work with those reported in literature [12].
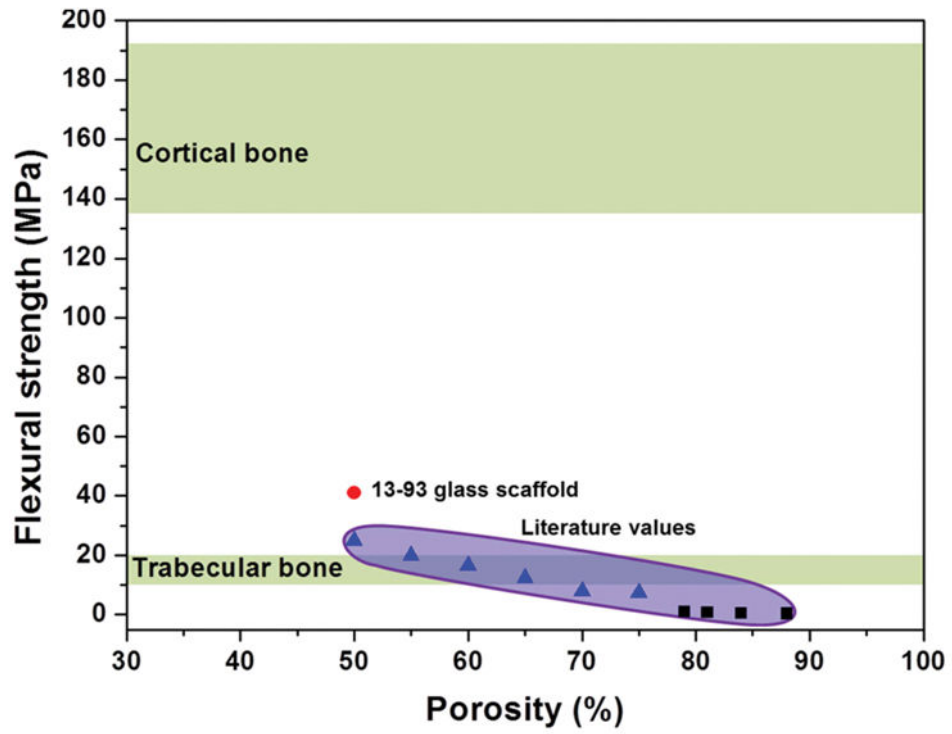
Figure 6.
(a) Stress-strain curve of the scaffold under 3-point bending; (b) SEM image of a fracture surface in PCL-coated scaffold after bending test. Insets showing the stress-strain curve at a small strain level and the loading direction relative to the pore orientation during the test.
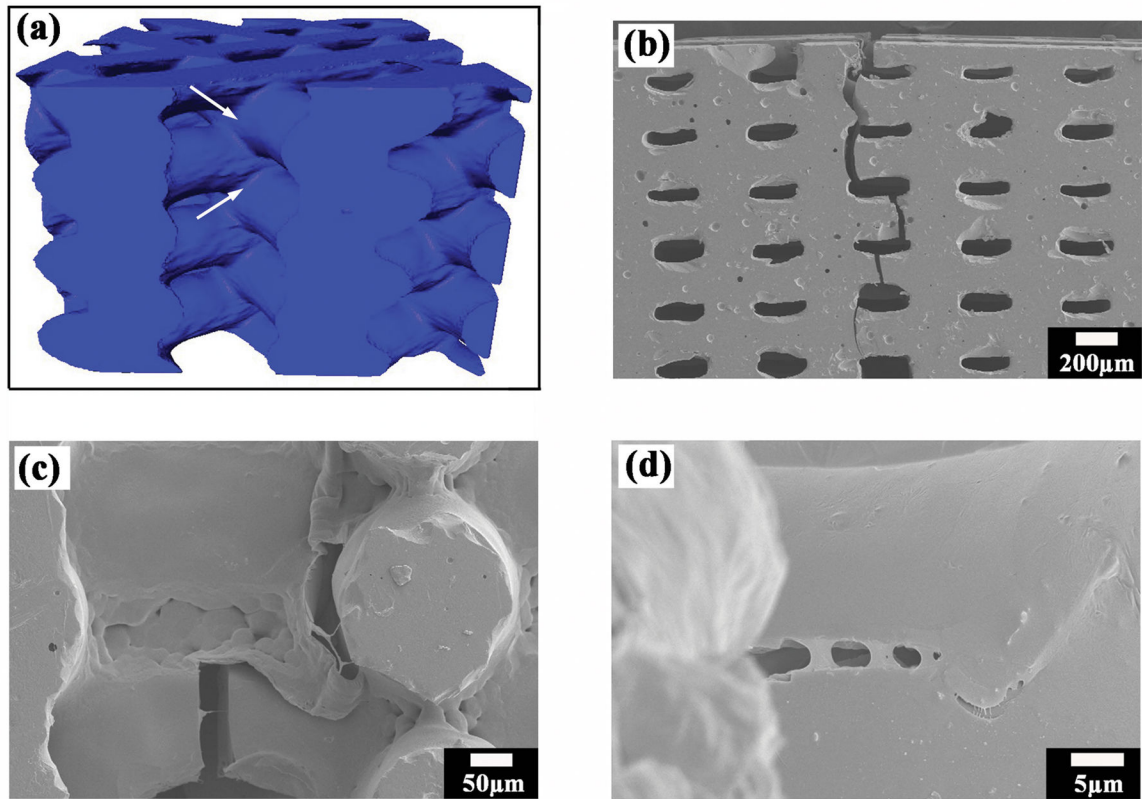
Figure 7.
(a) Weibull distribution of flexural strength of uncoated and PCL-coated glass scaffolds; (b) logarithmic plots for flexural strength values of both scaffolds

Figure 8.
A comparison of flexural strength of bioactive glass in this work with those reported in literature [12].

Figure 9.
(a) A 3-dimensional view of the joining of adjacent glass struts using synchrotron X-ray tomography; (b) crack propagation path in a pre-cracked un-coated glass scaffold; (c) crack propagation path in a pre-cracked PCL-coated glass scaffold; (d) PCL fibril elongation in coated glass scaffold after bending test.

Table 1

Mechanical strength, toughness and reliability of uncoated and PCL-coated 13–93 glass scaffold. Significant difference was observed in compressive strength between uncoated and PLC-coated scaffolds, but not in flexural strength or fracture toughness. Statistical analysis with one-way analysis of variance(ANOVA) followed by a Tukey's *post hoc* test, with the level of significance set at p < 0.05.

Scaffold	Uncoated 13–93 scaffold	PCL-coated 13–93 scaffold
Compressive strength, MPa	80 ± 10	102 ± 11
Young's modulus, GPa	4.7 ± 0.5	3.9 ± 0.4
Weibull modulus (compression)	6.0 ± 0.5	13.0 ± 1.0
Flexural strength, MPa	40 ± 5	41 ± 6
Weibull modulus (bending)	5.3 ± 0.4	5.6 ± 0.5
Fracture toughness (K_{IC}), MPa·m$^{1/2}$	0.8 ± 0.2	0.8 ± 0.2